

Article

Synthesis of Lipase-Immobilized CeO₂ Nanorods as Heterogeneous Nano-Biocatalyst for Optimized Biodiesel Production from *Eruca sativa* Seed Oil

Anam Fatima ¹, Muhammad Waseem Mumtaz ^{1,*}, Hamid Mukhtar ², Sadia Akram ¹,
Tooba Touqeer ¹, Umer Rashid ^{3,*}, Muhammad Raza Ul Mustafa ^{4,5},
Imededdine Arbi Nehdi ^{6,7} and Mohd Izham Saiman ^{8,9}

¹ Department of Chemistry, University of Gujrat, Gujrat 50700, Pakistan; anam.cheema.uog@gmail.com (A.F.); sadia.nano@yahoo.com (S.A.); tuba.toqir@gmail.com (T.T.)

² Institute of Industrial Biotechnology, Government College University, Lahore 54000, Pakistan; hamidwaseer@yahoo.com

³ Institute of Advanced Technology, Universiti Putra Malaysia, Serdang 43400 UPM, Malaysia

⁴ Department of Civil and Environmental Engineering, Universiti Teknologi PETRONAS, Seri Iskandar 32610, Malaysia; raza.mustafa@utp.edu.my

⁵ Centre for Urban Resource Sustainability, Institute of Self-Sustainable Building, Universiti Teknologi PETRONAS, Seri Iskandar 32610, Malaysia

⁶ Chemistry Department, College of Science, King Saud University, Riyadh 11451, Saudi Arabia; inahdi@ksu.edu.sa

⁷ Laboratoire de Recherche LR18ES08, Chemistry Department, Science College, Tunis El Manar University, Tunis 2092, Tunisia

⁸ Catalysis Science and Technology Research Centre, Faculty of Science, Universiti Putra Malaysia, Serdang 43400, Malaysia; mohdizham@upm.edu.my

⁹ Department of Chemistry, Faculty of Science, Universiti Putra Malaysia, Serdang 43400, Malaysia

* Correspondence: muhammad.waseem@uog.edu.pk (M.W.M.); umer.rashid@upm.edu.my (U.R.); Tel.: +60-3-9769-7393 (U.R.)

Received: 6 November 2019; Accepted: 2 December 2019; Published: 15 February 2020



Abstract: Biodiesel has emerged as one of the most attractive alternative energy sources to meet the growing needs of energy. Many approaches have been adopted for biodiesel synthesis. In the present work, biodiesel was produced from non-edible *Eruca sativa* oil using nano-biocatalyst-catalysed transesterification. Nano-biocatalyst (CeO₂@PDA@*A. terreus* Lipase) was developed via the immobilization of lipase on polydopamine coated ceria nanorods, and CeO₂ nanorods were developed via a hydrothermal process. The mean diameter of nanorods were measured to be 50–60 nm, while their mean length was 150–200 nm. Lipase activity before and after immobilization was measured to be 18.32 and 16.90 U/mg/min, respectively. The immobilized lipase depicted high stability at high temperature and pH. CeO₂@PDA@*A. terreus* Lipase-catalysed transesterification resulted in 89.3% yield of the product. Process optimization through response surface methodology was also executed, and it was depicted that the optimum/maximum *E. sativa* oil-based biodiesel yield was procured at conditions of 10% CeO₂@PDA@*A. terreus* Lipase, 6:1 methanol/oil ratio, 0.6% water content, 35 °C reaction temperature, and 30 h reaction time. The fuel compatibility of synthesized biodiesel was confirmed via the estimation of fuel properties that were in agreement with the ASTM D standard. The nanorods and dopamine-modified nanorods were characterized by FTIR spectroscopy, SEM, and energy dispersive X-ray (EDX), while conversion of *E. sativa* oil to biodiesel was confirmed by GC/MS and FTIR spectroscopy. Conclusively, it was revealed that CeO₂@PDA@*A. terreus* Lipase has potential to be employed as an emphatic nano-biocatalyst.

Keywords: CeO₂ nanorods; polydopamine; *Aspergillus terreus* Lipase; biodiesel; optimization

1. Introduction

Depletion of petroleum reservoirs has stimulated the scientific community worldwide to search for alternate energy resources. Biodiesel has notable potential as an imperative green fuel [1]. The additional impacts of biodiesel production are to increase agricultural production and productivity, to increase the income of rural communities, to lessen pollution, and to create new jobs [2]. Biodiesel is a biodegradable, relatively nontoxic, and green fuel with reduced CO and unburned hydrocarbons (UHC) emission. Moreover, biodiesel has benefits such as appropriate lubricity, and no sulphur [3]. Biodiesel is widely manufactured using the transesterification process, which is catalyzed by numerous catalysts. Transesterification lowers the viscosity of feedstock oils [4] which reacts with alcohol, resulting in biodiesel. Many acidic and basic catalysts have been employed for the said purpose, but enzymatic catalysis is being promoted. The chemical methods of transesterification are considered to be problematic due to the production of poor-quality glycerol, the production of alkaline wastes, washing requirements, side reactions, and issues related to biodiesel recovery and purification. Therefore, enzymes are preferred over chemical catalysts in the transesterification to prepare biodiesel [5].

Various lipases are frequently being used in the transesterification process. It has been observed that the reproducibility and catalytic activity of immobilized enzymes are better than the non-immobilized enzymatic system [6]. Immobilization also makes the enzyme reusable and stable. Different microbial lipases have been immobilized on various surfaces, such as gels, ceramics, and alginates beads [7]. Recently, nanoparticles have also gained much attraction as effective supports for enzyme immobilization. Nanoparticles of a very small size provide a large surface area for enzyme immobilization, and characteristic Brownian motion of nanoparticles provide higher enzymatic activity [8]. Lipases are mostly immobilized on magnetic nanoparticles; other supports used for this purpose are nanoparticles of silver, magnesium, and carbon nanotubes. Successful immobilization of lipase on nano-materials/supports in biodiesel synthesis enhances the efficiency of the transesterification process and makes lipase reusable, which finally reduces the cost of the process without compromising the yield and quality [9]. The production of biodiesel from nano-immobilized lipase involves (1) the preparation of enzyme; (2) the synthesis of nanoparticles (NPs); (3) the attachment of enzyme with nanomaterials, directly or through suitable a linkage or mediator; and (4) the transesterification of feedstock oil using synthesized nano-biocatalyst [10]. Bearing in mind the significance of nano-immobilized lipase, this work was planned to develop CeO₂-based nano-biocatalyst for the synthesis of fatty acid methyl esters/biodiesel from *E. sativa* oil.

2. Results and Discussion

2.1. Scanning Electron Microscopy (SEM)-Based Characterization

From the SEM micrographs (Figure 1a,b), it can be seen that the morphology of prepared CeO₂ is rod-like. These nanorods are uniform in shape and size, and they are not agglomerated. At different magnification levels, the SEM images revealed that the nanorods have mean diameter of 50–60 nm, whereas their mean length was 150–200 nm.

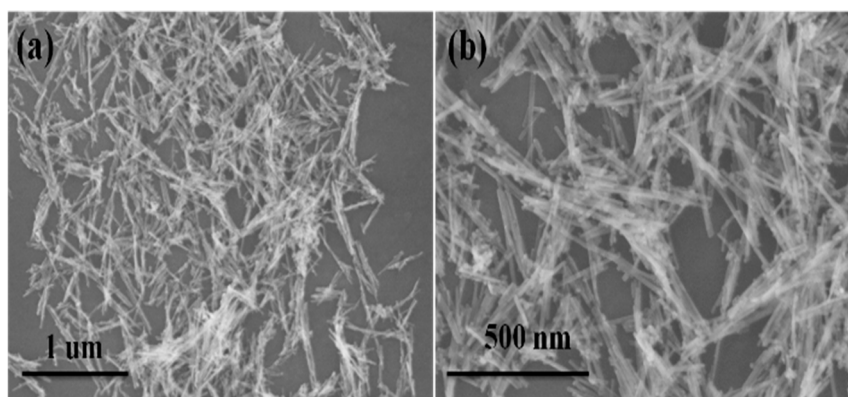


Figure 1. SEM micrographs of CeO₂ nanorods (a) low resolution, 1 μm (b) high resolution, 500 nm.

2.2. Energy Dispersive X-Ray Spectroscopy (EDX)

The constituent elements of the nanorods were determined using energy dispersive X-ray (EDX) spectroscopy. The plot between energy of X-rays vs. X-rays counts is presented in (Figure 2). Each peak in the plot corresponds to a specific element. EDX plot confirms the presence of cerium and oxygen in the product. Absence of extra peaks may be attributed to the purity of synthesized nanorods, while peak for carbon is due to the carbon plates of instrument. Atomic% and weight% of elements obtained by EDX are shown in Table 1. Ratio of atomic% between cerium and oxygen affirms the formation of CeO₂ nanorods.

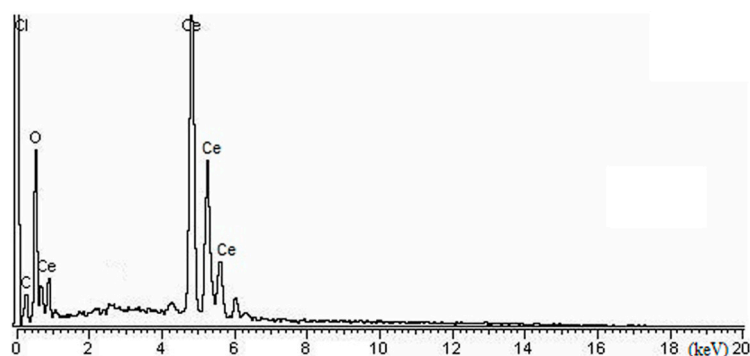


Figure 2. EDX analysis of CeO₂ nanorods.

Table 1. Constituent elements of CeO₂ nanorods.

Element	Weight%	Atomic%
C	4.99	21.62
O	17.76	50.88
Ce	77.25	27.50
Totals	100.00	100.00

2.3. X-Ray Diffraction (XRD)

XRD pattern (Figure 3) was used to characterize the CeO₂ nano-powder, and instrument was operated within range of 20–80°. The peaks appeared in the XRD pattern with 2θ values at 27.95°, 32.71°, 46.93°, 56.21°, 59.27°, and 69.03°, ascribed to the d-values (with cubic phase) 0.319 (111), 0.275 (200), 0.194 (220), 0.164 (311), 0.156 (222), and 0.136 (400), respectively. The XRD pattern of CeO₂ nanorods was in fine arrangement with the standard JCPDS card no# (JCPDS-34-0394). The spectrum indicates that there are no additional impurity peaks present.

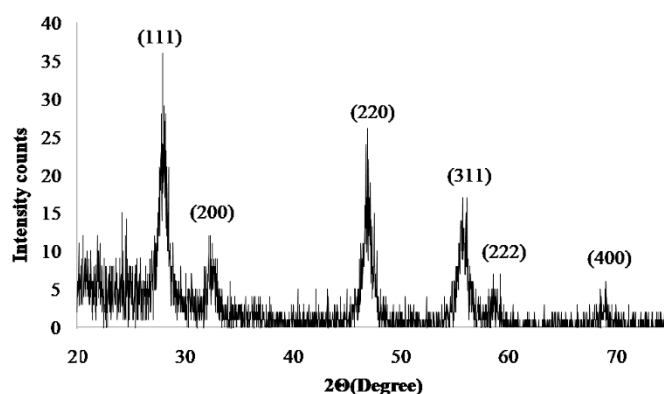


Figure 3. XRD pattern of CeO₂ nanorods.

2.4. Fourier Transform Infrared Spectroscopic (FTIR) Analysis of Naked and Polydopamine Coated CeO₂ Nanorods

Both the polydopamine-coated and uncoated CeO₂ nanorods were scanned for FTIR spectroscopy in the range of 600–4000 cm⁻¹ (Figure 4). FTIR spectrum (blue colored) reveals the functional groups and the chemical bonds that are present in the synthesized, uncoated CeO₂ nanorods, whereas FTIR (black colored) spectrum confirms the functionalization of CeO₂ nanorods with polydopamine layer. The broad band at 3402.47 cm⁻¹ corresponds to (the stretching vibration of O-H bond) OH-groups. The peak around 1569.67 cm⁻¹ is ascribed to the bending vibration of N-H group. The absorption peak around 1496.92 cm⁻¹ indicates the -CH₂ vibrations. The intense band at 691.17 cm⁻¹ corresponds to the Ce-O stretching vibrations [11]; another additional peak at 1312.27 cm⁻¹ corresponds to the C-O bonds in dopamine molecule that verifies the dopamine addition on CeO₂ nanorods [12].

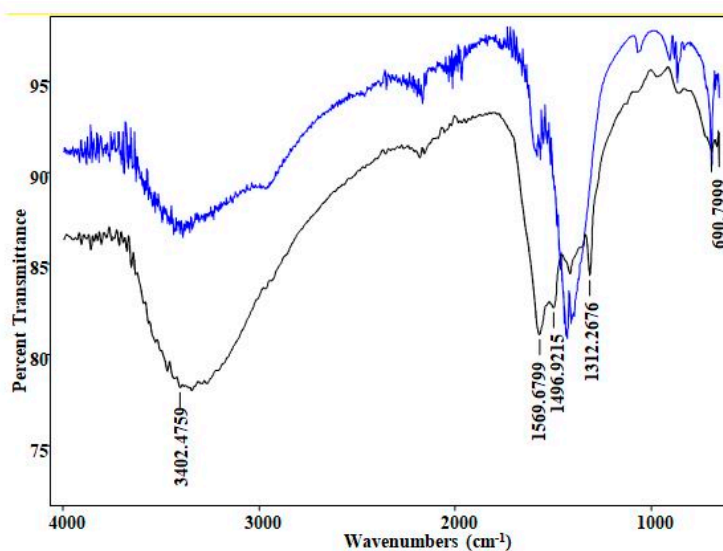


Figure 4. FTIR of CeO₂ and polydopamine-coated CeO₂ nanorods.

2.5. Lipase Activity Assay

The activity titer of free lipase (which was produced from *Aspergillus terreus* AH-F2) was found to be 18.32 U/mg/min, while the activity titer of CeO₂@PDA@*A. terreus* Lipase was found to be 16.90 U/mg/min. It was found that, by using polydopamine, high immobilization efficiency was achieved by using CeO₂ nanorods because polydopamine and CeO₂ nanorods formed the complex, which was found to be efficient regarding immobilization of lipase. The wider surface was available during the reaction, which gave higher conversion rate in a short period of time by using the lipase-immobilized nanorods for

biodiesel production [13]. To the best of our knowledge, the synthesized nano-biocatalyst with CeO₂ nanorods as immobilizing support for Lipase (*Aspergillus terreus* AH-F2) may be novel nano-biocatalyst for biodiesel synthesis.

2.6. Effect of pH and Temperature on Activity of Nano-Biocatalyst

The impact of pH on the activity of free lipase and synthesized nano-biocatalyst is presented in (Figure 5a). The effect of pH was studied within pH range of 5 to 10, and it was found that maximum lipase activity, i.e., 18.32 U/mg/min, was observed at pH 7.0 in case of free lipase, while at pH 8, CeO₂@PDA@*A. terreus* Lipase showed maximum activity (i.e., 16.90 U/mg/min). The relationship plot between activities of Lipase (Free and immobilized) and pH depicted that CeO₂@PDA@*A. terreus* Lipase could tolerate high pH values. The comparison of free and immobilized lipase revealed that immobilizing *A. terreus* Lipase on CeO₂@PDA increased the flexibility of lipase to a wide pH range, compared to free lipase. Our results were comparable to the studies of Baharfar and Mahajer [13].

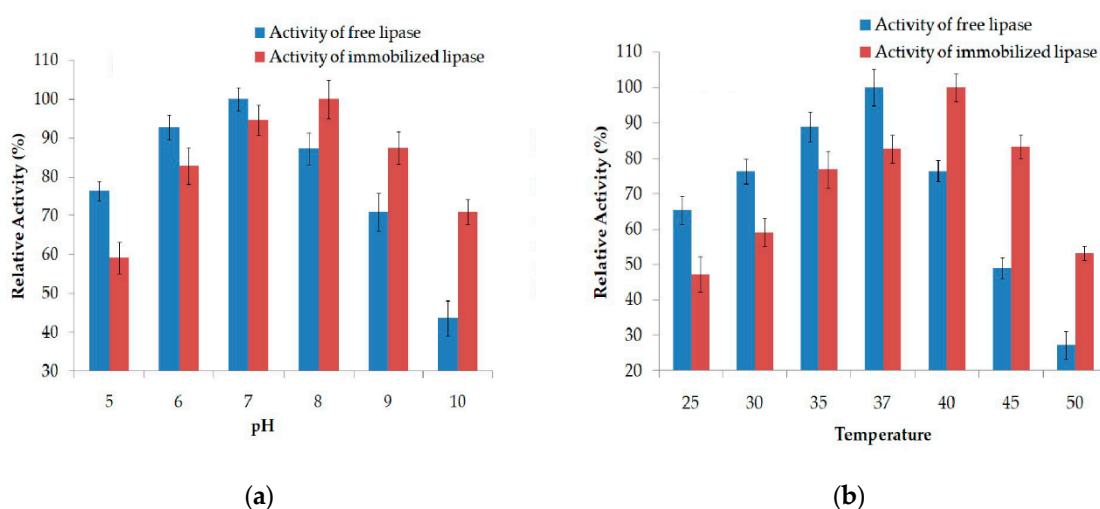


Figure 5. (a) The impact of pH on the activity of free lipase and synthesized nano-biocatalyst at 37 °C and (b) the impact of temperature on the activity of free lipase and synthesized nano-biocatalyst at pH 7.

The impact of temperature (ranging from 25 to 50 °C) on the activity of free lipase (*A. terreus* Lipase) and CeO₂@PDA@*A. terreus* Lipase is presented in Figure 5b. It was depicted that highest free lipase activity was revealed at 30 °C, while the CeO₂@PDA@*A. terreus* Lipase showed highest/maximum activity at 40 °C, so it showed that CeO₂@PDA@*A. terreus* Lipase was tolerant to high temperature conditions and was stable at a wider temperature range. The increased tolerability of lipase may have been due to the formation of covalent bonds during immobilization. Comparable observations have been reported by Baharfar & Mahajer [13] and Dumri & Hung [14].

2.7. Physico-Chemical Properties of *E. sativa* Seed Oil

Physico-chemical properties of *E. sativa* oil are described below in (Table 2). Density is measure of mass per unit value of a sample (*E. sativa* oil) [15]. Peroxide value is the measure of amount of peroxides in the sample, i.e., oil or fats [16]. The ratio of density of sample to the water density is described by specific gravity [17]. Acid value is the amount of potassium hydroxide (mg) required for the deactivation of the fatty acids present in the 1.0 g of sample (oil) [18]. Iodine value is the measurement of unsaturation in the given oil; if the iodine value is high, then degree of unsaturation is high. The milligram of KOH required to saponify each gram of oil under specific set of conditions is referred as saponification value [19].

Table 2. Physico-chemical characteristics/properties of *E. sativa* oil.

Sr#	Physicochemical Property	Units	Value
1	Density	(g/cm ³)	0.81 ± 0.29
2	Peroxide value	(meq)	3.97 ± 0.163
3	Specific gravity	g/cm ³	0.75 ± 0.0041
4	Acid value	(mg KOH/g)	1.197 ± 0.0058
5	Iodine value	mg/g	102.17 ± 0.671
6	Saponification value	mg KOH/g	5.36 ± 1.70

2.8. Biodiesel Yield (%) and Optimum Reaction Conditions

Optimum reaction conditions for CeO₂@PDA@*A. terreus* Lipase-catalyzed transesterification of *E. sativa* are given below in (Table 3), with maximum biodiesel yield of 89.3%. Optimum reaction conditions revealed were reaction time (30 h), temperature (35 °C), alcohol/oil ratio (6:1), water content (0.6%), and CeO₂@PDA@*A. terreus* Lipase concentration (10%). The same enzyme (*A. terreus* Lipase) has also been immobilized on magnetite nano-support in another study performed by our research group, and comparable reaction conditions were revealed for optimal biodiesel production (92%) with slight variation in reaction temperature (37 °C). When methanol is added in oil, the viscosity of oil decreases and reaction rate increases, which is why methanol is significant for the reaction rate, but if an excessive amount of methanol is added in oil then emulsification of the glycerol may take place, deactivating the lipase and minimizing the biodiesel yield [20].

Table 3. Optimum reaction conditions for biodiesel production.

Catalyst	Reaction Time (hours)	Reaction Temp (°C)	Methanol: Oil Ratio	Water (%)	Catalyst Conc. (%)	Yield (%)
CeO ₂ @PDA@ <i>A. terreus</i> Lipase	30	35	6:1	0.6	10	89.3

The other factor is catalyst concentration that influences the reaction rate. In the current study, 10% CeO₂@PDA@*A. terreus* Lipase concentration was observed as optimum concentration for the synthesis of *E. sativa* seed oil-based biodiesel. The maximum yield of biodiesel (89.3%) may be increased by taking higher concentration of nano-biocatalyst or by using different lipase source for immobilization on functionalized CeO₂. Another factor is reaction temperature, when the reaction is carried out at a more optimum temperature than reaction rate and biodiesel yield is maximum. However, high temperature denatured the lipase and reduced the biodiesel yield. Water content is also significant for the reaction rate, as it affects the activity and stability of lipase and protects it from deactivation via short chain alcohols [21].

Previously different researchers have employed response surface methodology (RSM) for biodiesel production using various feedstock oils and catalysts [22,23]. Aghababaie et al. has described bio-catalytic biodiesel synthesis from the crude *E. sativa* oil and obtained the highest FAME yield at 3:1 methanol to oil ratio, 5 mg lipase, 40% water content, and 21 °C temperature. The results that have been reported in literature are comparable to the present work [24–27], but still some variations are present that might be due to the varying fatty acid profiles of feedstock, different activities of the catalysts, and ranges of reaction parameters selected for optimization process.

2.9. RSM Model Fitting

Central composite design was applied to optimize biodiesel production procedure. Among the different models (viz; linear, quadratic, cubic polynomial, and two-factor interaction 2FI), quadratic model was revealed to be the most significant model for the responses with *p*-value < 0.0001 for CeO₂@PDA@*A. terreus* Lipase catalyzed transesterification of sample oil. Fitness of quadratic model

was also confirmed by the lack of fitness test, which was insignificant for the model with p -value 0.0728 in addition to higher R^2 and adjusted R^2 values (Table 4).

Table 4. Response surface methodology (RSM) model fitting for optimization of *E. sativa* oil-based biodiesel.

Feedstock	Catalyst	Selected Model	Model Significance (p -Value)	R^2 Value	Adj. R^2 Value	Lack of Fit
<i>Eruca sativa</i> seed oil	CeO ₂ @PDA@ <i>A. terreus</i> Lipase	Quadratic	<0.0001	0.9802	0.9903	0.0728

Fitness of the model was also affirmed by the normality and predicted vs. actual values graph (Figure 6). The linear distribution of data along the straight line in normality plot of the model depicts the fitness of quadratic models, while the small difference b/w predicted, and actual values of biodiesel yield further advocates the significance of quadratic models.

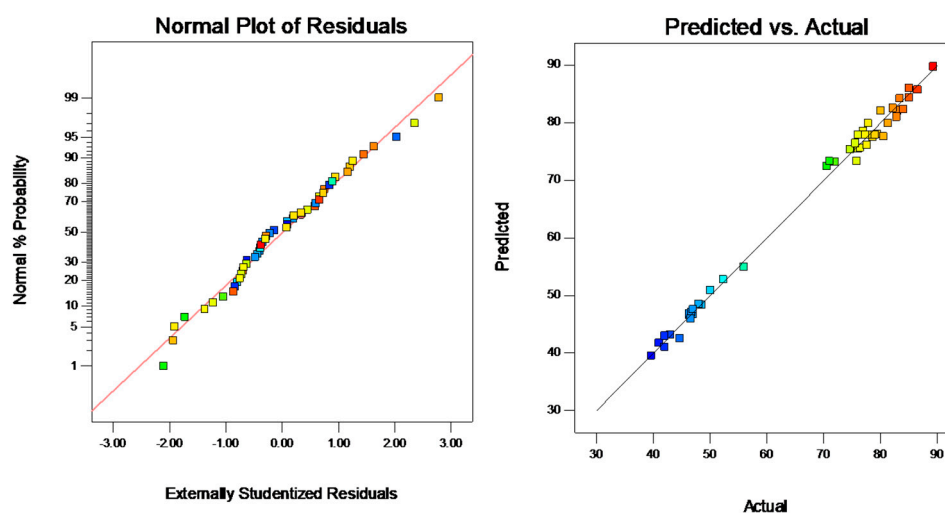


Figure 6. Normality plot of residuals for model and correlation graph between predicted and actual values.

2.10. ANOVA for Biodiesel Yield Response

Table 5 represents the ANOVA for the selected quadratic model describing the impact of various reaction parameters (as linear terms, 1st order interaction and quadratic terms) on response (% biodiesel yield) catalyzed by CeO₂@PDA@*A. terreus* Lipase.

A (methanol/oil ratio), B (CeO₂@PDA@*A. terreus* Lipase concentration), and D (reaction time) were significant linear terms, while C and E were non-significant (>0.05) with p -value 0.1344 and 0.6091, respectively. The AB, AC, AE, and BC were significant interaction terms, having p -values of 0.0069, 0.0283, 0.0243, and 0.0013, respectively (<0.05). As for the quadratic terms, quadratic terms B², C², and D² were the most significant quadratic terms, with p -values of 0.0001, 0.0001, and 0.0240, respectively, while A² and E² were non-significant quadratic terms that had p -values > 0.05.

Comparable results have been obtained in previous research. Mehmood et al. (2018) described the ANOVA for the significant quadratic model for biodiesel production from *E. sativa* oil catalysed by H₂SO₄ and reported that A (amount of catalyst) and D (methanol/oil ratio) impact significantly on the response (biodiesel yield), while B (temperature) and C (time) were non-significant terms. Regarding the 1st order interaction terms, BC and CD were significant, whereas AB, AC, AD, and BD were non-significant. Among the quadratic terms, D² and B² were significant [28].

Table 5. ANOVA for biodiesel yield response.

Source	Sum of Squares	Df	Mean Square	F Value	p-Value
Model	12,774.84	20	638.74	251.87	<0.0001
Methanol to oil ratio (A)	182.17	1	182.17	71.83	<0.0001
Enzyme conc. (B)	10,283.40	1	10,283.40	4054.96	<0.0001
Reaction temp. (C)	6.01	1	6.01	2.37	0.1344
Reaction time (B)	157.17	1	157.17	61.97	<0.0001
Water content (E)	0.68	1	0.68	0.27	0.6091
A × B	21.45	1	21.45	8.46	0.0069
A × C	13.52	1	13.52	5.33	0.0283
A × D	1.53	1	1.53	0.60	0.4434
A × E	14.31	1	14.31	5.64	0.0243
B × C	32.00	1	32.00	12.62	0.0013
B × D	9.46	1	9.46	3.73	0.0632
B × E	0.061	1	0.061	0.024	0.8776
C × D	0.020	1	0.020	7.886×10^3	0.9298
C × E	0.020	1	0.020	7.886×10^3	0.9298
D × E	3.25	1	3.25	1.28	0.2668
A ²	0.11	1	0.11	0.044	0.8352
B ²	75.16	1	75.16	29.64	<0.0001
C ²	62.14	1	62.14	24.50	<0.0001
D ²	14.40	1	14.40	5.68	0.0240
E ²	6.04	1	6.04	2.38	0.1337
Residual	73.54	29	2.54		
Lack of Fit	66.39	22	3.02	2.95	0.0728
Pure Error	7.16	7	1.02		
Cor Total	12,848.38	49			

Mumtaz et al. also reported the ANOVA for bio-catalytic synthesis of palm oil-based biodiesel. According to their findings, linear terms that showed a significant effect on response (% biodiesel) were A (amount of bio-catalyst), B (reaction time), and D (methanol/oil ratio). Among first-order interacting terms, AD showed significant influence on biodiesel yield. Among quadratic terms, B² and D² were depicted to be significant [29]. In another previous study, Chang et al. reported the analysis of variance for experimental data obtained by Lipase catalyzed biodiesel production from Novozym 435. The significant linear terms were X₂ (reaction temperature), X₃ (enzyme concentration), X₄ (substrate molar ratio), and X₅ (water content), while the non-significant term was X₁ (reaction time) [30].

Razack and Durairasan also reported ANOVA for the biodiesel production from waste cooking oil catalyzed by encapsulated mixed enzyme in which the only significant linear factor was C (reaction temperature); while A (enzyme), B (molar ratio) and D(time) had *p*-value > 0.05. Significant quadratic factors were revealed to be A², B², and C². AC was the only significant first order interaction term [31].

The results reported previously are comparable with the results obtained in present work with some variation. The significance of methanol-to-oil ratio and enzyme concentration is obvious, as they directly influence the reaction rate. The enzymatic transesterification is a slow process so the significance of reaction time for enzymatic transesterification cannot be denied, as reported by other researchers as well [32]. Water is also considered as an imperative factor; however, water concentration (as linear term) has not been proved significant in the present work.

2.11. 3D Surface Graphs for % Biodiesel Yield

Response surface plots of interaction terms depicting significant influence on response (biodiesel yield) are presented in (Figure 7). 3D graph describing the cumulative impact of CeO₂@PDA@*A. terreus* Lipase and CH₃OH/oil ratio indicated that the % biodiesel increases with an increase in nano-biocatalyst level and methanol/oil ratio, and optimal biodiesel yield is obtained when nano-biocatalyst level and

methanol/oil ratio were 10% and 6:1, respectively. Deviation from these values, however, results in lower biodiesel yield. 3D graph between temperature and methanol/oil ratio showing their impact on response is shown in (Figure 7b), which shows that the highest response was observed at 6:1 methanol/oil ratio and 35 °C reaction temperature. However, high temperature can denature the active sites of the enzyme. Response surface plot for methanol-to-oil ratio and water content is presented in Figure 7c, which predicts that the combination of these two variables also affect the response. Figure 7d shows the combined effect of temperature and nano-biocatalyst concentration on the response, which indicates that the yield rises with rise in reaction temperature and nano-biocatalyst amount until it reaches an optimum point, i.e., 35 °C and 10%, respectively, while beyond this point a decline in % biodiesel yield is observed.

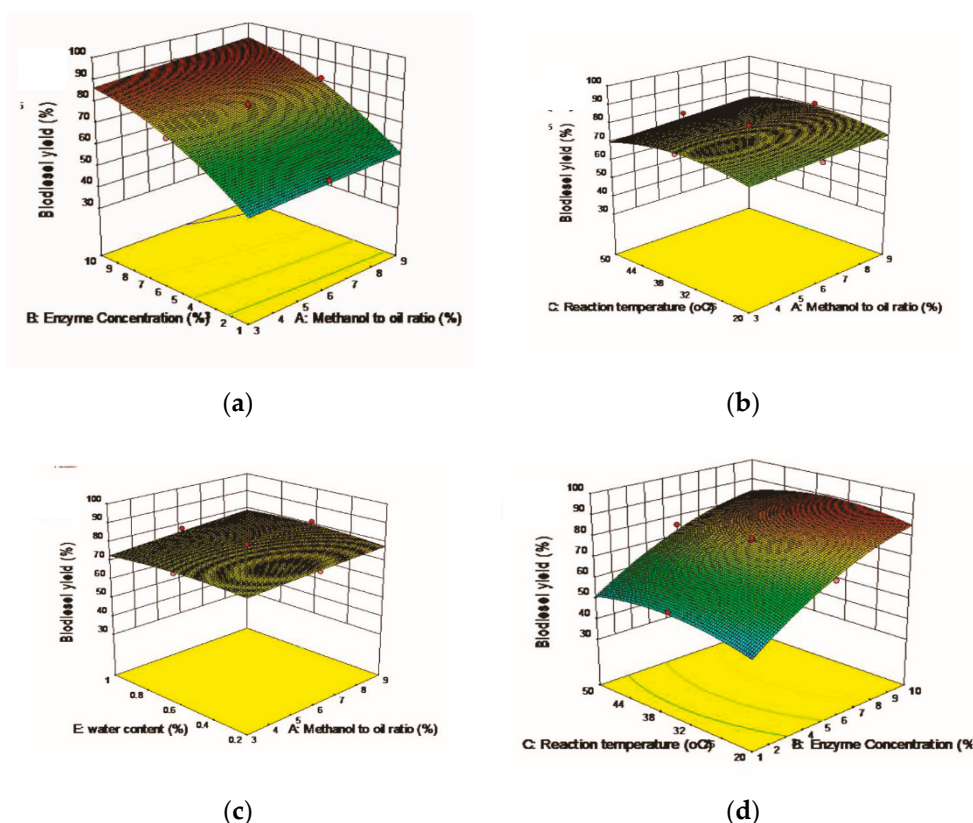


Figure 7. 3D graphical plots describing the impact of significant first-order interactions between (a) enzyme concentration \times methanol to oil ratio (b) reaction temperature \times methanol to oil ratio (c) water content \times methanol to oil ratio (d) reaction temperature \times enzyme concentration on biodiesel yield nano-biocatalyst reactions.

2.12. FTIR Spectroscopic Analysis of *Eruca Sativa* Oil and Biodiesel

The transesterification of *E. sativa* oil and biodiesel was monitored by FTIR spectroscopy (Figure 8). The IR absorption band at 1438.0935 cm^{-1} corresponds to the $-\text{CH}_3$ asymmetric bending that was present in *E. sativa* oil-based biodiesel but absent in *E. sativa* oil FTIR spectra. Similarly, absorption band at 1196.7202 cm^{-1} ascribed to $\text{O}-\text{CH}_2$ stretching which was absent in *E. sativa* oil but present in *E. sativa* biodiesel spectra. The bands at 1161.1 cm^{-1} , 1459.3 cm^{-1} , and 1099.6 cm^{-1} , corresponding to $\text{C}-\text{O}$ stretching, $\text{C}=\text{C}$ stretching, and OCH_2C asymmetric stretching, respectively, were absent in *E. sativa* oil biodiesel but present in *E. sativa* oil FTIR spectra. The bands at $1700\text{--}1800\text{ cm}^{-1}$ and $2800\text{--}3000\text{ cm}^{-1}$ (vibrational frequency band of $\text{C}=\text{O}$ stretching and CH_2 symmetric stretching, respectively) were present in both *E. sativa* oil and *E. sativa* oil biodiesel spectra. Tariq et al. reported the conversion of *E. sativa* oil into biodiesel by disappearance of peaks in *E. sativa* oil at 1465 and 1095 cm^{-1} and formation

of new peaks at 1435 and 1195 cm^{-1} in the biodiesel [33]. Similar results have been reported in other research [34].

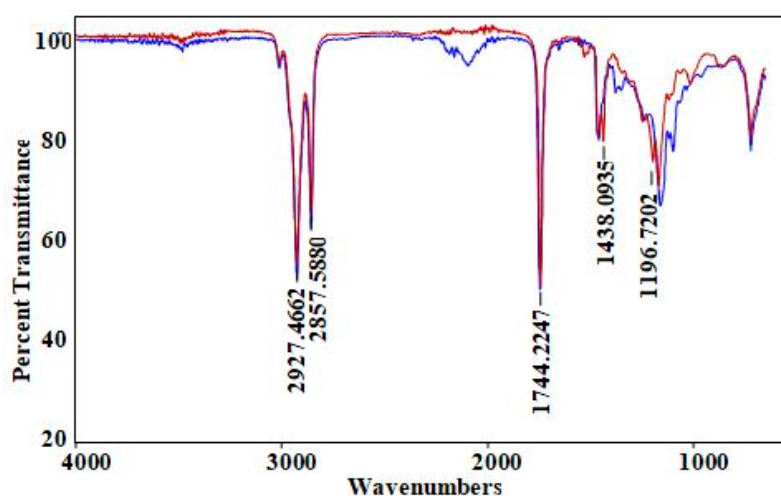


Figure 8. FTIR spectrum of *E. sativa* oil and biodiesel.

2.13. Major Fatty Acid Methyl Esters of Synthesized Biodiesel

GC-MS analysis for the profiling of major fatty acids methyl esters in product (biodiesel) is presented in (Table 6). Palmitic acid (1.448% composition), oleic acid (28.181% composition), stearic acid (0.186%), gondoic acid (4.712%), and erucic acid (65.111%) were the major fatty acid methyl esters identified in sample.

Table 6. Major FAMES of biodiesel.

Peak #	Retention Time (mints)	Fatty Acid	Percentage (%)
1	14.5991	Palmitic acid (16:0)	1.448 ± 0.012
2	18.896	Oleic acid (18:1)	28.181 ± 0.432
3	17.8101	Stearic acid (18:0)	0.186 ± 0.002
4	20.30	Gondoic acid (20:1)	4.712 ± 0.132
5	25.9340	Erucic acid (22:0)	65.111 ± 1.44

Mumtaz et al. reported the fatty acids profile of *E. sativa* oil that consists of palmitic acid (2.8%), linoleic acid (10.3%), stearic acid (0.90%), oleic acid (16.3%), linolenic acid (12.56%), and erucic acid (47.7%) [35]. Chakrabarti and Ahmad also investigated and reported palmitic acid (10.2%), stearic acid (1.6%), oleic acid (22.8%), linoleic acid (6.4%), linolenic acid (11.9%), and erucic acid (40.8%) as major fatty acids in *E. sativa* oil [36].

2.14. Recovery and Reusability of Nano-Biocatalyst

Centrifugation was used to recover the nano-biocatalyst, which was then examined for lipase activity. It was revealed that after first use, there was no change in the $\text{CeO}_2\text{@PDA@A. terreus}$ Lipase activity, i.e., 16.90 U/mg/min (Table 7). So, recovered $\text{CeO}_2\text{@PDA@A. terreus}$ Lipase was reused multiple times for the production of biodiesel and after each reuse, the activity of lipase was assayed, which showed that a considerable decrease in the activity of lipase was observed after five uses, and after seven uses the activity was decreased to 3.9 U/mg/min. The immobilization of lipase is important for the economy of the biodiesel production process, as was observed/revealed by the results. The nano-biocatalyst can be used up to five times without significant decrease in activity, while free enzymes are readily deactivated at high temperatures, with little variations in pH and in the presence of short-chain alcohols, especially methanol [20]. So nano-immobilized lipases can appreciably help

in cost reduction of biodiesel production process. After five uses, the biodiesel synthesis rate was reduced, which might have been due to the contact of nano-biocatalyst to organic compounds present in the reaction mixture during biodiesel production or recurring contact with heat. Similar studies have also been reported by Dumri and Hung [14].

Table 7. Reusability of lipase-immobilized on CeO₂ nanorods.

Cycles	Lipase Activity U/mg/min
1	16.9 ± 0.4
2	16.7 ± 0.5
3	16 ± 0.4
4	12.3 ± 0.7
5	11.0 ± 0.52
6	7.1 ± 0.08
7	4.4 ± 0.1
8	3.9 ± 0.3

2.15. Fuel Characteristics

Biodiesel fuel properties/characteristics were evaluated based on standard methods. The estimated fuel properties values of *E. sativa*-based biodiesel are presented in (Table 8).

Table 8. Fuel properties of biodiesel.

Properties	Unit	Value	ASTM D Std
Flash point	°C	192.4 ± 1.9	>130
Pour point	°C	−3.22 ± 0.51	−15 to 16
Cloud point	°C	−10 ± 0.018	−3 to −12
Fire point	°C	208.5 ± 1.4	>130
Kinematic viscosity	mm ² /s	5.2 ± 0.3	1.9–6.0 mm ² /sec

3. Materials and Methods

Research/analytical grade chemicals were used in the whole experimental work. CeNO₃·6H₂O, NaOH, ethanol, lipase, methanol, acetone, polydopamine, phosphate buffer, tris-HCl buffer, and phenolphthalein were obtained from Sigma Chemical Co. (St. Louis, MO, USA). *Eruca sativa* seeds were obtained from Directorate of Land Reclamation Agriculture Department, Lahore, Pakistan.

3.1. Preparation of CeO₂ Nanorods

CeO₂ nanorods were prepared by using the hydrothermal method, during which 7.2 g of NaOH was dissolved in 20.0 mL distilled H₂O along with stirring in a beaker. In another beaker, 2.17 g of CeNO₃·6H₂O was dissolved in 10 mL distilled H₂O. Then, the aqueous solution of CeNO₃·6H₂O was added dropwise in the above solution of NaOH with continuous stirring. After 10 min, white precipitates were obtained. Then, the mixture was filled in 60 mL Teflon lined autoclave and kept in oven for 24 h at 120 °C. Light-yellow-colored product was acquired that was washed with distilled H₂O and ethanol. For calcination, the dried product was also kept in furnace for 2 h at 500 °C [37].

3.2. Coating of Dopamine on CeO₂ Nanorods

For dopamine coating on CeO₂ nanorods, 0.3 g of prepared CeO₂ nanorods was dispersed in 20 mL of distilled H₂O in a flask, then 20 mL of 20 mM tris buffer having pH 8.5 was added in the flask. 0.1 g of polydopamine was added in the above mixture and stirred for 1 h. The obtained suspension was separated by centrifugation and washed with the tris-HCl buffer to remove the unwanted polydopamine. Addition of polydopamine on nanorods was due to the polymerization of dopamine in the basic conditions [38].

3.3. Characterization of CeO₂ Nanorods

CeO₂ nanorods were characterized by means of the SEM, XRD, FT-IR, and EDX spectroscopy. XRD pattern for CeO₂ nanorods was obtained by using the X'pertpro (PANalytical) with radiations of Cu k alpha of wavelength 1.54 Å in the scan range of 20–80°, 2θ with scan step size of 0.02. XRD gave the information about the particle size, crystal phase, and dimensions of CeO₂ nanorods. The particle size and surface morphology of CeO₂ nanorods were confirmed by using the scanning electron microscope (JSM5910, JEOL, Tokyo, Japan) with 30 kV energy, (300,000×) maximum magnification, and 2.3 nm resolving power. The formation of CeO₂ nanorods and their modification with polydopamine were performed by using the Cary 630 Agilent FT-IR spectroscopy. EDX gives information about the purity, composition, and elemental analysis of the CeO₂ nanorods. EDX spectroscopic analysis was performed using EDX (JSM5910) (INCA200/Oxford instruments, High Wycombe, UK).

3.4. Immobilization of Lipase on Modified Nanorods

0.4 g of lipase was added in the 40 mL of phosphate buffer. The mixture of polydopamine-coated nanorods was slowly added in the lipase mixture with continuous stirring for 3 h at 4 °C. The resulting nano-biocatalyst (CeO₂@PDA@*A. terreus* Lipase) was washed with the phosphate buffer several times to remove the un-reacted lipase and dried in desiccator at low temperature [39]. Figure 9 shows the lipase immobilization process. The immobilization efficiency was revealed by investigating the protein content in solution (before and after immobilization) using Bradford's method.

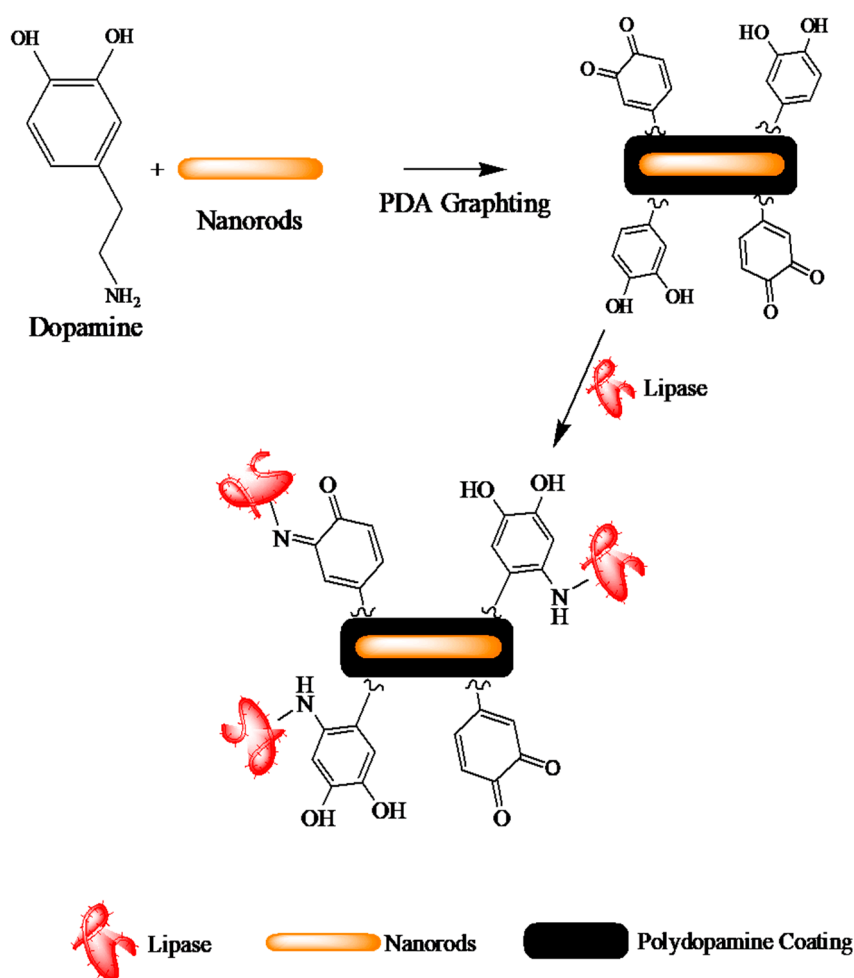


Figure 9. Schematic presentation of lipase immobilization process.

3.5. Lipase Activity Assay in Free and Immobilized Form

Titrimetric method was performed for free and immobilized lipase activity assay [40]. The assay mixtures consisted of specific amounts of nano-biocatalysts, along with 10 mL of homogeneous mixture of olive oil in gum acacia, 5 mL of phosphate buffer (pH 7), and 2.0 mL of CaCl₂ (0.6%); then, the mixture was incubated at 37 °C for 1 h. Afterward, the reaction was stopped using 20 mL of ethanol:acetone (1:1) followed by the titration with 0.1 N NaOH solution. The lipase activity assay was executed by the titration of fatty acids produced from olive oil after reaction with the lipase.

One unit of lipase activity was defined as “the amount of enzyme which released one micro mole (μmol) of fatty acid per min. under specified assay conditions”.

Lipase units were determined as follows:

$$\text{Lipase Activity} = (\Delta V \times N \times 1000)/M \times 60 \quad (1)$$

where $\Delta V = V_2 - V_1$; V_1 = vol. of NaOH used against control flask; V_2 = vol. of NaOH used against experimental flask; N = normality of NaOH; $M(\text{sample})$ = mass of enzyme extract; and 60 = time of incubation (min) for bacterial lipase.

3.6. Effect of pH and Temperature on Activity of Free and Immobilized Enzyme

The effects of temperature and pH were studied on the activity of free lipase (*A. terreus* Lipase) and immobilized lipase (CeO₂@PDA@*A. terreus* Lipase). The impact of temperature in the range of 25 to 50 °C and the pH in the range of 5 to 10 (using phosphate buffer) were investigated. Reactions were performed in triplicates.

3.7. Collection of Feedstock, Extraction of Oil, and Its Quality Assessment

The *Eruca sativa* seeds were subjected to solvent extraction based on Soxhlet technique for the extraction of oil using hexane as solvent. The extracted *E. sativa* seed oil was analyzed for its initial quality check by evaluating its iodine value, peroxide value, viscosity, acid value, specific gravity, and saponification value by means of AOCS standard protocols [35].

3.8. Central Composite Response Surface Methodology (CCRSM) Experimental Design

CCRSM was used for optimized biodiesel production from CeO₂@PDA@*A. terreus* Lipase catalyzed transesterification of *E. sativa* oil. Five independent variables—A (methanol/oil ratio), B (biocatalyst amount), C (reaction temperature), D (reaction period), and E (water content)—were optimized within the ranges 3:1–9:1, 1–10%, 20 °C–50 °C, 12–48 h, and 0.2–1%, respectively. Fifty reactions were performed as per CCRD experimental design. In a typical biodiesel production reaction, a conical flask was used containing the reaction mixture oil, methanol, bio-catalyst, and distilled H₂O. The reaction conditions were set according to the RSM experimental design. When the reactions were completed, glycerol was separated from biodiesel. Biodiesel was washed with warm water and using the rotary evaporator the residual methanol was recovered under the reduced-pressure conditions.

The model used for response surface methodology is given below:

$$Y_{\text{yield}} = b_0 + \sum_{i=1}^k b_i X_i + \sum_{i=1}^k b_i X_i^2 + \sum_{i=1}^k \sum_{\substack{j=1 \\ i > j}}^k b_{ij} X_i X_j + e \quad (2)$$

3.9. Recovery and Recycling of CeO₂@PDA@*A. Terreus* Lipase

After completion of transesterification reactions, the nano-biocatalyst (CeO₂@PDA@*A. terreus* Lipase) was recovered by centrifugation of glycerol and methyl esters. The recovered nano-biocatalyst was washed with water, dried in air, and reused for transesterification to produce biodiesel [41].

3.10. Characterization of Biodiesel

The resulted biodiesel was characterized by FTIR spectroscopic and gas chromatographic techniques. Fuel properties were also determined using standard ASTM methods [42]. Fourier transform infrared spectroscopic analysis was performed by using the Cary 630 Agilent FTIR spectrometer for the *E. sativa* oil and biodiesel in the range of 400–4000 cm^{-1} .

Gas chromatography-mass spectrometry (GC-MS) analysis was carried out for the estimation of fatty acids methyl ester in the synthesized biodiesel. For this purpose, GCMS QP 2010 instrument dB 5 column of diameter 0.15 mm was used. Sample size and split ratio were 1 μL and 1:100, respectively. Helium was the carrier gas, and 1.2 mL/min flow rate was selected for sample elution. Oven temperature was set between 150 to 250 $^{\circ}\text{C}$, at rate of 4 $^{\circ}\text{C}$ per minute. MS mass scanning range was 30–550 m/z . NIST MS library of GCMS was used to identify the alkyl esters. Biodiesel produced was further analyzed according to ASTM D methods to estimate the fuel properties to check their suitability as fuel.

Gas chromatography was performed using polar BPX_70 capillary column 30 m \times 0.25 mm and FID detector, to determine biodiesel yield/ester content. Helium at 1.5 mL/min flow rate was used as carrier gas. The column oven temperature was kept at 100 $^{\circ}\text{C}$ and then increased to 260 $^{\circ}\text{C}$, at rate of 10 $^{\circ}\text{C}/\text{min}$. 1 g sample was taken in hexane having methyl heptadecanoate as internal standard, and 1 μL of this mixture was injected in column. FAME (%) yield was determined by using the following formula:

$$\text{FAME (\%)} = \frac{\sum \text{AME} - A}{A} \times \frac{C \times V}{M} \times 100 \quad (3)$$

where $\sum A_{\text{ME}}$ denotes the sum of peak areas of all FAMAs. A is the peak area of methyl heptadecanoate, C is the concentration of the internal standard, V is the volume of the internal standard, and M is mass of biodiesel.

4. Conclusions

In the current study, $\text{CeO}_2@\text{PDA}@A. terreus$ Lipase was utilized for conversion of *E. sativa* oil into methyl esters and the optimization of process through response surface methodology was carried out. 89.3% FAME yield was obtained by carrying out reactions under optimum conditions of 10% $\text{CeO}_2@\text{PDA}@A. terreus$ Lipase, 6:1 methanol/oil ratio, and 0.6% water at 35 $^{\circ}\text{C}$ for 30 h reaction time. The fuel properties of synthesized product (biodiesel) were compatible with ASTM standards. $\text{CeO}_2@\text{PDA}@A. terreus$ Lipase was ascertained to exhibit efficient catalytic characteristics. Hence, $\text{CeO}_2@\text{PDA}@A. terreus$ Lipase may further be explored for the transesterification of other feedstock to attain a maximum yield of environmentally friendly fuel.

Author Contributions: A.F., M.W.M., and U.R. conceived of this article; the methodology was designed by A.F., M.W.M., and U.R.; the writing—original draft was prepared by A.F.; S.A., T.T., and M.W.M., who also helped with the editing and supervision. H.M. helped in lipase immobilization studies and I.A.N., U.R., and M.R.U.M. reviewed the manuscript for final version improvement. M.I.S. also helped to revise the manuscript. All authors have read and agreed to the published version of the manuscript.

Acknowledgments: The authors acknowledge their gratitude to King Saud University (Riyadh, Saudi Arabia) for the support of this research through Researchers Supporting Project number (RSP-2019/80).

Conflicts of Interest: The author declares no conflict of interest.

References

1. Srivastava, A.; Prasad, R. Triglycerides-based diesel fuels. *Renew. Sustain. Energy Rev.* **2000**, *4*, 111–133. [[CrossRef](#)]
2. Thornhill, S.; Vargyas, E.; Fitzgerald, T.; Chisholm, N. Household food security and biofuel feedstock production in rural Mozambique and Tanzania. *Food Secur.* **2016**, *8*, 953–971. [[CrossRef](#)]

3. Soltani, S.; Rashid, U.; Yunus, R.; Taufiq-Yap, Y.H. Biodiesel production in the presence of sulfonated mesoporous ZnAl₂O₄ catalyst via esterification of palm fatty acid distillate (PFAD). *Fuel* **2016**, *178*, 253–262. [[CrossRef](#)]
4. Peng, B.X.; Shu, Q.; Wang, J.F.; Wang, G.R.; Wang, D.Z.; Han, M.H. Biodiesel production from waste oil feedstocks by solid acid catalysis. *Process Saf. Environ. Prot.* **2008**, *86*, 441–447. [[CrossRef](#)]
5. Rashid, U.; Rehman, H.A.; Hussain, I.; Ibrahim, M.; Haider, M.S. Muskmelon (*Cucumis melo*) seed oil: A potential non-food oil source for biodiesel production. *Energy* **2011**, *36*, 5632–5639. [[CrossRef](#)]
6. Karimi, M. Immobilization of lipase onto mesoporous magnetic nanoparticles for enzymatic synthesis of biodiesel. *Biocatal. Agric. Biotechnol.* **2016**, *8*, 182–188. [[CrossRef](#)]
7. Adlercreutz, P. Immobilisation and application of lipases in organic media. *Chem. Soc. Rev.* **2013**, *42*, 6406–6436. [[CrossRef](#)]
8. Al-Zuhair, S.; Dowaidar, A.; Kamal, H. Dynamic modeling of biodiesel production from simulated waste cooking oil using immobilized lipase. *Biochem. Eng. J.* **2009**, *44*, 256–262. [[CrossRef](#)]
9. Xie, W.; Wang, J. Enzymatic production of biodiesel from soybean oil by using immobilized lipase on Fe₃O₄/poly (styrene-methacrylic acid) magnetic microsphere as a biocatalyst. *Energy Fuel.* **2014**, *28*, 2624–2631. [[CrossRef](#)]
10. Jamil, F.; Al-Haj, L.; Ala'a, H.; Al-Hinai, M.A.; Baawain, M.; Rashid, U.; Ahmad, M.N.M. Current scenario of catalysts for biodiesel production: A critical review. *Rev. Chem. Eng.* **2018**, *34*, 267–297. [[CrossRef](#)]
11. Ali, M.M.; Mahdi, H.S.; Parveen, A.; Azam, A. Optical properties of cerium oxide (CeO₂) nanoparticles synthesized by hydroxide mediated method. *AIP Conf. Proc.* **2018**, *1953*, 030044.
12. Arumugam, A.; Karthikeyan, C.; Hameed, A.S.H.; Gopinath, K.; Gowri, S.; Karthika, V. Synthesis of cerium oxide nanoparticles using *Gloriosasuperba*, L. leaf extract and their structural, optical and antibacterial properties. *Mater. Sci. Eng. C* **2015**, *49*, 408–415. [[CrossRef](#)] [[PubMed](#)]
13. Baharfar, R.; Mohajer, S. Synthesis and Characterization of Immobilized Lipase on Fe₃O₄ Nanoparticles as Nano biocatalyst for the Synthesis of Benzothiazepine and Spirobenzothiazine Chroman Derivatives. *Catal. Lett.* **2016**, *146*, 1729–1742. [[CrossRef](#)]
14. Dumri, K.; Hung Anh, D. Immobilization of Lipase on Silver Nanoparticles via Adhesive Polydopamine for Biodiesel Production. *Enzym. Res.* **2014**, *2014*, 389739. [[CrossRef](#)] [[PubMed](#)]
15. Nayak, P.K.; Dash, U.; Rayaguru, K.; Krishnan, K.R. Physio-chemical changes during repeated frying of cooked oil: A review. *J. Food Biochem.* **2016**, *40*, 371–390. [[CrossRef](#)]
16. Li, S.; Wang, Y.; Dong, S.; Chen, Y.; Cao, F.; Chai, F.; Wang, X. Biodiesel production from *Eruca Sativa* Gars vegetable oil and motor, emissions properties. *Renew. Energy* **2009**, *34*, 1871–1876. [[CrossRef](#)]
17. Idun-Acquah, N.; Obeng, G.Y.; Mensah, E. Repetitive use of vegetable cooking oil and effects on physico-chemical properties—Case of frying with redfish (*Lutjanusfulgens*). *Sci. Technol.* **2016**, *6*, 8–14.
18. Sahoo, P.K.; Das, L.M.; Babu, M.K.G.; Naik, S.N. Biodiesel development from high acid value polanga seed oil and performance evaluation in a CI engine. *Fuel* **2007**, *86*, 448–454. [[CrossRef](#)]
19. Gopinath, A.; Puhan, S.; Nagarajan, G. Theoretical modeling of iodine value and saponification value of biodiesel fuels from their fatty acid composition. *Renew. Energy* **2009**, *34*, 1806–1811. [[CrossRef](#)]
20. Christopher, L.P.; Kumar, H.; Zambare, V.P. Enzymatic biodiesel: Challenges and opportunities. *Appl. Energy* **2014**, *119*, 497–520. [[CrossRef](#)]
21. Korkut, I.; Bayramoglu, M. Selection of catalyst and reaction conditions for ultrasound assisted biodiesel production from canola oil. *Renew. Energy* **2018**, *116*, 543–551. [[CrossRef](#)]
22. Mumtaz, M.W.; Mukhtar, H.; Dilawer, U.A.; Hussain, S.M.; Hussain, M.; Iqbal, M.; Nisar, J. Biocatalytic transesterification of *Eruca sativa* oil for the production of biodiesel. *Biocatal. Agric. Biotechnol.* **2016**, *5*, 162–167. [[CrossRef](#)]
23. Eevera, T.; Rajendran, K.; Saradha, S. Biodiesel production process optimization and characterization to assess the suitability of the product for varied environmental conditions. *Renew. Energy* **2009**, *34*, 762–765. [[CrossRef](#)]
24. Aghababaie, M.; Beheshti, M.; Razmjou, A.; Bordbar, A.K. Enzymatic biodiesel production from crude *Eruca sativa* oil using *Candida rugosa* lipase in a solvent-free system using response surface methodology. *Biofuels* **2017**, *1–7*. [[CrossRef](#)]
25. Chai, F.; Cao, F.; Zhai, F.; Chen, Y.; Wang, X.; Su, Z. Transesterification of vegetable oil to biodiesel using a heteropolyacid solid catalyst. *Adv. Synth. Catal.* **2007**, *349*, 1057–1065. [[CrossRef](#)]

26. Xie, W.; Huang, M. Immobilization of *Candida rugosa* lipase onto graphene oxide Fe₃O₄ nanocomposite: Characterization and application for biodiesel production. *Energy Convers. Manag.* **2018**, *159*, 42–53. [[CrossRef](#)]
27. Ahmad, T.; Danish, M.; Kale, P.; Geremew, B.; Adeloju, S.B.; Nizami, M.; Ayoub, M. Optimization of process variables for biodiesel production by transesterification of flaxseed oil and produced biodiesel characterizations. *Renew. Energy* **2019**, *139*, 1272–1280. [[CrossRef](#)]
28. Mehmood, T.; Fareed, S.; Iqbal, M.; Naseem, A.; Siddique, F. Utilization of Agro-waste and Non-conventional *Eruca sativa* Seed Oil for Getting Optimized Process to Acquire Better Yield of Biodiesel by Using Response Surface Methodology (RSM). *Chiang Mai J. Sci.* **2018**, *45*, 1507–1518.
29. Mumtaz, M.W.; Mukhtar, H.; Anwar, F.; Saari, N. RSM based optimization of chemical and enzymatic transesterification of palm oil: Biodiesel production and assessment of exhaust emission levels. *Sci. World J.* **2014**, *2014*, 526105. [[CrossRef](#)]
30. Chang, H.M.; Liao, H.F.; Lee, C.C.; Shieh, C.J. Optimized synthesis of lipase-catalyzed biodiesel by Novozym 435. *J. Chem. Technol. Biotechnol. Int. Res. Process Environ. Clean Technol.* **2005**, *80*, 307–312. [[CrossRef](#)]
31. Razack, S.A.; Durairasan, S. Response surface methodology assisted biodiesel production from waste cooking oil using encapsulated mixed enzyme. *Waste Manag.* **2016**, *47*, 98–104. [[CrossRef](#)] [[PubMed](#)]
32. Tan, T.; Lu, J.; Nie, K.; Deng, L.; Wang, F. Biodiesel production with immobilized lipase: A review. *Biotechnol. Adv.* **2010**, *28*, 628–634. [[CrossRef](#)] [[PubMed](#)]
33. Tariq, M.; Ali, S.; Ahmad, F.; Ahmad, M.; Zafar, M.; Khalid, N.; Khan, M.A. Identification, FT-IR, NMR (1H and 13C) and GC/MS studies of fatty acid methyl esters in biodiesel from rocket seed oil. *Fuel Process. Technol.* **2011**, *92*, 336–341. [[CrossRef](#)]
34. Sherazi, S.T.H.; Arain, S.; Mahesar, S.A.; Bhangar, M.I.; Khaskheli, A.R. Erucic acid evaluation in rapeseed and canola oil by Fourier transform-infrared spectroscopy. *Eur. J. Lipid Sci. Technol.* **2013**, *115*, 535–540. [[CrossRef](#)]
35. Mumtaz, M.W.; Adnan, A.; Mahmood, Z.; Mukhtar, H.; Danish, M.; Ahmad, Z. Biodiesel production using *Eruca sativa* oil: Optimization and characterization. *Pak. J. Bot.* **2012**, *44*, 1111–1120.
36. Chakrabarti, M.H.; Ahmad, R.A.F.I.Q. Investigating possibility of using least desirable edible oil of *Eruca sativa* L.; in biodiesel production. *Pak. J. Bot.* **2009**, *41*, 481–487.
37. Dhall, A.; Self, W. Cerium oxide nanoparticles: A brief review of their synthesis methods and biomedical applications. *Antioxidants* **2018**, *7*, 97. [[CrossRef](#)]
38. Nayak, P.; Santhosh, P.N.; Ramaprabhu, S. Cerium oxide nanoparticles decorated graphene nanosheets for selective detection of dopamine. *J. Nanosci. Nanotechnol.* **2015**, *15*, 4855–4862. [[CrossRef](#)]
39. Nwachukwu, E.; Ejike, E.; Ejike, B.; Onyeonula, E.; Chikezie-Abba, R.; Okorochoa, N.; Onukaogu, U.E. Characterization and Optimization of Lipase Production from Soil Microorganism (*Serratia marcescens*). *Int. J. Curr. Microbiol. Appl. Sci.* **2017**, *6*, 1215–1231. [[CrossRef](#)]
40. Shabbir, A.; Mukhtar, H. Optimization process for enhanced extracellular lipases production from a new isolate of *Aspergillus terreus* AH F-2. *Pak. J. Bot.* **2018**, *50*, 1571–1578.
41. Mukhtar, H.; Khursheed, S.; Ikram ul, H.; Mumtaz, M.W.; Rashid, U.; Al-Resayes, S.I. Optimization of Lipase Biosynthesis from *Rhizopus oryzae* for Biodiesel Production Using Multiple Oils. *Chem. Eng. Technol.* **2016**, *39*, 1707–1715. [[CrossRef](#)]
42. Singh, V.; Bux, F.; Sharma, Y.C. A low cost one pot synthesis of biodiesel from waste frying oil (WFO) using a novel material, β -potassium dizirconate (β -K₂Zr₂O₅). *Appl. Energy* **2016**, *172*, 23–33. [[CrossRef](#)]

